Eur. Phys. J. C (2005)
Digital Object Identifier (DOI) 10.1140/epjc/s2005-02323-9

THE EUROPEAN PHYSICAL JOURNAL C

Recent high-p_{T} results from STAR

C.A. Gagliardi[a] on behalf of the STAR Collaboration

J. Adams[3], M.M. Aggarwal[29], Z. Ahammed[43], J. Amonett[20], B.D. Anderson[20], D. Arkhipkin[13], G.S. Averichev[12], S.K. Badyal[19], Y. Bai[27], J. Balewski[17], O. Barannikova[32], L.S. Barnby[3], J. Baudot[18], S. Bekele[28], V.V. Belaga[12], A. Bellingeri-Laurikainen[38], R. Bellwied[46], J. Berger[14], B.I. Bezverkhny[48], S. Bharadwaj[33], A. Bhasin[19], A.K. Bhati[29], V.S. Bhatia[29], H. Bichsel[45], J. Bielcik[48], J. Bielcikova[48], A. Billmeier[46], L.C. Bland[4], C.O. Blyth[3], S. Blyth[21], B.E. Bonner[34], M. Botje[27], A. Boucham[38], J. Bouchet[38], A.V. Brandin[25], A. Bravar[4], M. Bystersky[11], R.V. Cadman[1], X.Z. Cai[37], H. Caines[48], M. Calderón de la Barca Sánchez[17], J. Castillo[21], O. Catu[48], D. Cebra[7], Z. Chajecki[28], P. Chaloupka[11], S. Chattopadhyay[43], H.F. Chen[36], Y. Chen[8], J. Cheng[41], M. Cherney[10], A. Chikanian[48], W. Christie[4], J.P. Coffin[18], T.M. Cormier[46], M.R. Cosentino[35], J.G. Cramer[45], H.J. Crawford[6], D. Das[43], S. Das[43], M. Daugherity[40], M.M. de Moura[35], T.G. Dedovich[12], A.A. Derevschikov[31], L. Didenko[4], T. Dietel[14], S.M. Dogra[19], W.J. Dong[8], X. Dong[36], J.E. Draper[7], F. Du[48], A.K. Dubey[15], V.B. Dunin[12], J.C. Dunlop[4], M.R. Dutta Mazumdar[43], V. Eckardt[23], W.R. Edwards[21], L.G. Efimov[12], V. Emelianov[25], J. Engelage[6], G. Eppley[34], B. Erazmus[38], M. Estienne[38], P. Fachini[4], J. Faivre[18], R. Fatemi[17], J. Fedorisin[12], K. Filimonov[21], P. Filip[11], E. Finch[48], V. Fine[4], Y. Fisyak[4], K.S.F. Fornazier[35], J. Fu[41], C.A. Gagliardi[39], L. Gaillard[3], J. Gans[48], M.S. Ganti[43], F. Geurts[34], V. Ghazikhanian[8], P. Ghosh[43], J.E. Gonzalez[8], H. Gos[44], O. Grachov[46], O. Grebenyuk[27], D. Grosnick[42], S.M. Guertin[8], Y. Guo[46], A. Gupta[19], T.D. Gutierrez[7], T.J. Hallman[4], A. Hamed[46], D. Hardtke[21], J.W. Harris[48], M. Heinz[2], T.W. Henry[39], S. Hepplemann[30], B. Hippolyte[18], A. Hirsch[32], E. Hjort[21], G.W. Hoffmann[40], M. Horner[21], H.Z. Huang[8], S.L. Huang[36], E.W. Hughes[5], T.J. Humanic[28], G. Igo[8], A. Ishihara[40], P. Jacobs[21], W.W. Jacobs[17], M Jedynak[44], H. Jiang[8], P.G. Jones[3], E.G. Judd[6], S. Kabana[2], K. Kang[41], M. Kaplan[9], D. Keane[20], A. Kechechyan[12], V.Yu. Khodyrev[31], J. Kiryluk[22], A. Kisiel[44], E.M. Kislov[12], J. Klay[21], S.R. Klein[21], D.D. Koetke[42], T. Kollegger[14], M. Kopytine[20], L. Kotchenda[25], K.L. Kowalik[21], M. Kramer[26], P. Kravtsov[25], V.I. Kravtsov[31], K. Krueger[1], C. Kuhn[18], A.I. Kulikov[12], A. Kumar[29], R.Kh. Kutuev[13], A.A. Kuznetsov[12], M.A.C. Lamont[48], J.M. Landgraf[4], S. Lange[14], F. Laue[4], J. Lauret[4], A. Lebedev[4], R. Lednicky[12], S. Lehocka[12], M.J. LeVine[4], C. Li[36], Q. Li[46], Y. Li[41], G. Lin[48], S.J. Lindenbaum[26], M.A. Lisa[28], F. Liu[47], H. Liu[36], J. Liu[34], L. Liu[47], Q.J. Liu[45], Z. Liu[47], T. Ljubicic[4], W.J. Llope[34], H. Long[8], R.S. Longacre[4], M. Lopez-Noriega[28], W.A. Love[4], Y. Lu[47], T. Ludlam[4], D. Lynn[4], G.L. Ma[37], J.G. Ma[8], Y.G. Ma[37], D. Magestro[28], S. Mahajan[19], D.P. Mahapatra[15], R. Majka[48], L.K. Mangotra[19], R. Manweiler[42], S. Margetis[20], C. Markert[20], L. Martin[38], J.N. Marx[21], H.S. Matis[21], Yu.A. Matulenko[31], C.J. McClain[1], T.S. McShane[10], F. Meissner[21], Yu. Melnick[31], A. Meschanin[31], M.L. Miller[22], N.G. Minaev[31], C. Mironov[20], A. Mischke[27], D.K. Mishra[15], J. Mitchell[34], B. Mohanty[43], L. Molnar[32], C.F. Moore[40], D.A. Morozov[31], M.G. Munhoz[35], B.K. Nandi[43], S.K. Nayak[19], T.K. Nayak[43], J.M. Nelson[3], P.K. Netrakanti[43], V.A. Nikitin[13], L.V. Nogach[31], S.B. Nurushev[31], G. Odyniec[21], A. Ogawa[4], V. Okorokov[25], M. Oldenburg[21], D. Olson[21], S.K. Pal[43], Y. Panebratsev[12], S.Y. Panitkin[4], A.I. Pavlinov[46], T. Pawlak[44], T. Peitzmann[27], V. Perevoztchikov[4], C. Perkins[6], W. Peryt[44], V.A. Petrov[46], S.C. Phatak[15], R. Picha[7], M. Planinic[49], J. Pluta[44], N. Porile[32], J. Porter[45], A.M. Poskanzer[21], M. Potekhin[4], E. Potrebenikova[12], B.V.K.S. Potukuchi[19], D. Prindle[45], C. Pruneau[46], J. Putschke[21], G. Rakness[30], R. Raniwala[33], S. Raniwala[33], O. Ravel[38], R.L. Ray[40], S.V. Razin[12], D. Reichhold[32], J.G. Reid[45], J. Reinnarth[38], G. Renault[38], F. Retiere[21], A. Ridiger[25], H.G. Ritter[21], J.B. Roberts[34], O.V. Rogachevskiy[12], J.L. Romero[7], A. Rose[21], C. Roy[38], L. Ruan[36], M.J. Russcher[27], R. Sahoo[15], I. Sakrejda[21], S. Salur[48], J. Sandweiss[48], M. Sarsour[17], I. Savin[13], P.S. Sazhin[12], J. Schambach[40], R.P. Scharenberg[32], N. Schmitz[23], K. Schweda[21], J. Seger[10], P. Seyboth[23], E. Shahaliev[12], M. Shao[36], W. Shao[5], M. Sharma[29], W.Q. Shen[37], K.E. Shestermanov[31], S.S. Shimanskiy[12], E Sichtermann[21], F. Simon[23], R.N. Singaraju[43], N. Smirnov[48], R. Snellings[27], G. Sood[42], P. Sorensen[21], J. Sowinski[17], J. Speltz[18], H.M. Spinka[1], B. Srivastava[32], A. Stadnik[12], T.D.S. Stanislaus[42], R. Stock[14], A. Stolpovsky[46], M. Strikhanov[25], B. Stringfellow[32], A.A.P. Suaide[35], E. Sugarbaker[28], C. Suire[4], M. Sumbera[11], B. Surrow[22], M. Swanger[10], T.J.M. Symons[21], A. Szanto de Toledo[35], A. Tai[8], J. Takahashi[35], A.H. Tang[27], T. Tarnowsky[32], D. Thein[8], J.H. Thomas[21], S. Timoshenko[25], M. Tokarev[12], T.A. Trainor[45], S. Trentalange[8], R.E. Tribble[39], O.D. Tsai[8], J. Ulery[32], T. Ullrich[4], D.G. Underwood[1], G. Van Buren[4], M. van Leeuwen[21], A.M. Vander Molen[24], R. Varma[16], I.M. Vasilevski[13], A.N. Vasiliev[31], R. Vernet[18], S.E. Vigdor[17], Y.P. Viyogi[43], S. Vokal[12], S.A. Voloshin[46], W.T. Waggoner[10], F. Wang[32], G. Wang[20], G. Wang[5], X.L. Wang[36], Y. Wang[40], Y. Wang[41], Z.M. Wang[36], H. Ward[40], J.W. Watson[20], J.C. Webb[17], G.D. Westfall[24], A. Wetzler[21], C. Whitten Jr.[8], H. Wieman[21], S.W. Wissink[17], R. Witt[2], J. Wood[8], J. Wu[36], N. Xu[21], Z. Xu[4],

[a] e-mail: cggroup@comp.tamu.edu

Z.Z. Xu[36], E. Yamamoto[21], P. Yepes[34], V.I. Yurevich[12], I. Zborovsky[11], H. Zhang[4], W.M. Zhang[20], Y. Zhang[36], Z.P. Zhang[36], R. Zoulkarneev[13], Y. Zoulkarneeva[13], A.N. Zubarev[12]

[1] Argonne National Laboratory, Argonne, Illinois 60439, USA
[2] University of Bern, 3012 Bern, Switzerland
[3] University of Birmingham, Birmingham, UK
[4] Brookhaven National Laboratory, Upton, New York 11973, USA
[5] California Institute of Technology, Pasadena, California 91125, USA
[6] University of California, Berkeley, California 94720, USA
[7] University of California, Davis, California 95616, USA
[8] University of California, Los Angeles, California 90095, USA
[9] Carnegie Mellon University, Pittsburgh, Pennsylvania 15213
[10] Creighton University, Omaha, Nebraska 68178
[11] Nuclear Physics Institute AS CR, 250 68 Řež/Prague, Czech Republic
[12] Laboratory for High Energy (JINR), Dubna, Russia
[13] Particle Physics Laboratory (JINR), Dubna, Russia
[14] University of Frankfurt, Frankfurt, Germany
[15] Institute of Physics, Bhubaneswar 751005, India
[16] Indian Institute of Technology, Mumbai, India
[17] Indiana University, Bloomington, Indiana 47408, USA
[18] Institut de Recherches Subatomiques, Strasbourg, France
[19] University of Jammu, Jammu 180001, India
[20] Kent State University, Kent, Ohio 44242, USA
[21] Lawrence Berkeley National Laboratory, Berkeley, California 94720, USA
[22] Massachusetts Institute of Technology, Cambridge, MA 02139-4307, USA
[23] Max-Planck-Institut für Physik, Munich, Germany
[24] Michigan State University, East Lansing, Michigan 48824, USA
[25] Moscow Engineering Physics Institute, Moscow Russia
[26] City College of New York, New York City, New York 10031, USA
[27] NIKHEF and Utrecht University, Amsterdam, The Netherlands
[28] Ohio State University, Columbus, Ohio 43210, USA
[29] Panjab University, Chandigarh 160014, India
[30] Pennsylvania State University, University Park, Pennsylvania 16802, USA
[31] Institute of High Energy Physics, Protvino, Russia
[32] Purdue University, West Lafayette, Indiana 47907, USA
[33] University of Rajasthan, Jaipur 302004, India
[34] Rice University, Houston, Texas 77251, USA
[35] Universidade de Sao Paulo, Sao Paulo, Brazil
[36] University of Science & Technology of China, Anhui 230027, P.R. China
[37] Shanghai Institute of Applied Physics, Shanghai 201800, P.R. China
[38] SUBATECH, Nantes, France
[39] Texas A&M University, College Station, Texas 77843, USA
[40] University of Texas, Austin, Texas 78712, USA
[41] Tsinghua University, Beijing 100084, P.R. China
[42] Valparaiso University, Valparaiso, Indiana 46383, USA
[43] Variable Energy Cyclotron Centre, Kolkata 700064, India
[44] Warsaw University of Technology, Warsaw, Poland
[45] University of Washington, Seattle, Washington 98195, USA
[46] Wayne State University, Detroit, Michigan 48201, USA
[47] Institute of Particle Physics, CCNU (HZNU), Wuhan 430079, P.R. China
[48] Yale University, New Haven, Connecticut 06520, USA
[49] University of Zagreb, Zagreb, 10002, Croatia

Received: 18 April 2005 / Revised version: 27 April 2005 /
Published online: 8 July 2005 –

Abstract. The STAR Collaboration has a broad range of recent results on intermediate and high-p_T phenomena in Au+Au collisions at $\sqrt{s_{NN}} = 200$ and 62 GeV and in d+Au at $\sqrt{s_{NN}} = 200$ GeV. These include new measurements of spectra, azimuthal anisotropies and di-hadron correlations. The comparison of the 62 and 200 GeV Au+Au results indicates that jet quenching, elliptic flow and di-hadron correlation measurements are very similar at the two energies. Meson-baryon differences that have been seen at intermediate p_T in 200 GeV Au+Au collisions are also present in 62 GeV Au+Au collisions and in 200

GeV d+Au collisions. Measurements of backward-forward inclusive hadron yield asymmetries and forward-midrapidity di-hadron correlations in d+Au collisions are consistent with the saturation picture. A brief review of these results is presented.

PACS. 25.75.Dw, 25.75.Ld, 25.75.Gz

1 Introduction

At RHIC, high transverse momentum (p_T) particles arise primarily from the fragmentation of energetic partons. In pp collisions at RHIC energies, high-p_T particle production can be well understood in terms of perturbative QCD. In heavy-ion collisions, energetic partons are produced very early in the collision. They then interact with the surrounding dense medium as they escape the collision zone. Thus, they can be used to probe the dense medium that is created in RHIC collisions [1].

Initial results from RHIC demonstrate that high-p_T inclusive hadron yields [2–4] and back-to-back di-hadron correlations [5] are strongly suppressed in central Au+Au collisions relative to pp collisions. In contrast, inclusive hadron yields are slightly enhanced in d+Au collisions relative to pp collisions, and back-to-back di-hadron correlations are very similar [6]. Thus, the high-p_T suppression seen in central Au+Au collisions arises from final-state interactions in the dense medium that is created in Au+Au collisions at RHIC. Calculations that attribute the suppression to partonic energy loss – "jet quenching" – have been successful in describing these data if they assume the initial density of the system is ~ 50 times that of normal nuclear matter. At intermediate p_T, meson yields are suppressed in central Au+Au collisions far more than baryons, and the elliptic flow values follow a meson-baryon rather than particle mass dependence [7–9]. These meson-baryon differences have been identified as signatures for hadronization through constituent quark recombination or coalescence [10]. In the forward direction, negative hadron yields are strongly suppressed in central d+Au collisions relative to peripheral d+Au or pp collisions [11], which may provide evidence for the onset of gluon saturation in Au nuclei at small-x. See [12] for a review of the results from the first three years of RHIC.

In this paper, we describe recent intermediate- and high-p_T results from STAR [13]. New spectra, azimuthal anisotropy, and di-hadron correlation measurements are available for $\sqrt{s_{NN}} = 200$ and 62 GeV Au+Au collisions and $\sqrt{s_{NN}} = 200$ GeV d+Au collisions. These results extend our understanding of the behavior of dense QCD matter at RHIC.

2 Spectra

Figure 1 shows a comparison of the inclusive charged hadron yields in central Au+Au collisions at 62, 130 and 200 GeV as measured by STAR, together with 17 GeV measurements for inclusive π^0 in central Pb+Pb collisions by WA98 [14]. The high-p_T yield drops far more rapidly at 62 GeV than it does at the higher collision energies. For

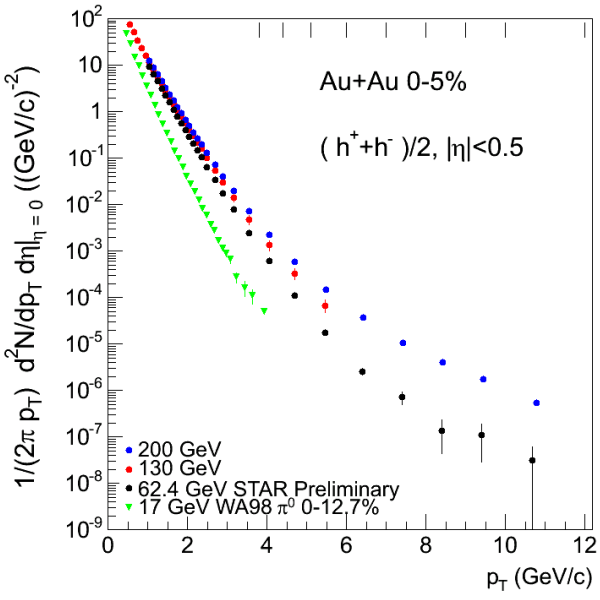

Fig. 1. Preliminary inclusive charged hadron yields in central Au+Au collisions at 62 GeV, compared to previous data at 130 and 200 GeV from STAR [2,3] and at 17 GeV from WA98 [14]

$p_T > 6$ GeV/c, the inclusive charged hadron yield is over a factor of 10 smaller at 62 GeV than at 200 GeV. This is the most interesting region to assess the evidence for jet quenching at 62 GeV because the baryon-meson differences at 200 GeV appear to vanish for $p_T > 6$ GeV/c [7–9]. Figure 2 shows the nuclear modification factor, R_{AA}, for Au+Au collisions at 62 and 200 GeV. R_{AA} at 62 GeV shows a significant enhancement in peripheral collisions. This may arise from the Cronin effect, which should be stronger at 62 GeV than 200 GeV due to the more steeply falling spectrum. R_{AA} indicates that high-p_T inclusive yields in central Au+Au collisions are suppressed at 62 GeV, though perhaps not as strongly as they are at 200 GeV. There is considerable uncertainty in the high-p_T nucleon-nucleon reference spectrum at 62 GeV that is required to compute R_{AA} [15]. Figure 3 shows R_{CP}, the relative yields in central vs. peripheral collisions, at 62 and 200 GeV. R_{CP} eliminates the uncertainty associated with the choice of reference spectrum. Figure 3 indicates that the suppression at intermediate p_T is not as strong at 62 GeV as was observed at 200 GeV; at high p_T, the behavior at the two energies is qualitatively similar. These 62 GeV results are consistent with calculations based on partonic energy loss [16].

STAR has also measured identified particle distributions in 62 GeV Au+Au collisions. The combination of tra-

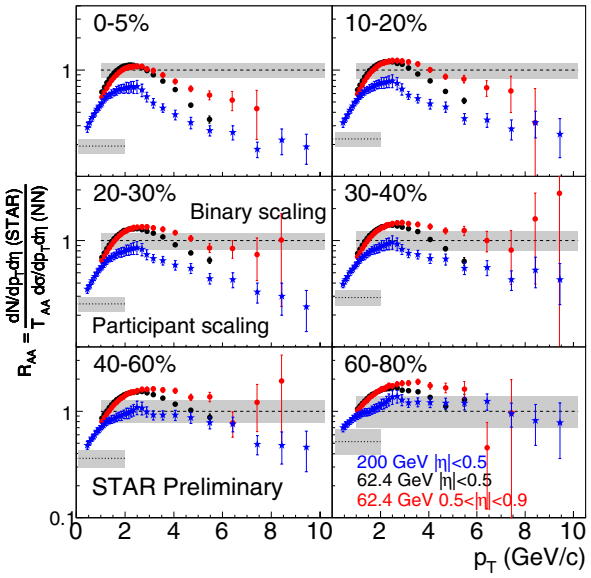

Fig. 2. Preliminary R_{AA} measurements at 62 GeV (circles) for two different pseudorapidity regions are compared to previous results at 200 GeV (stars) [3]

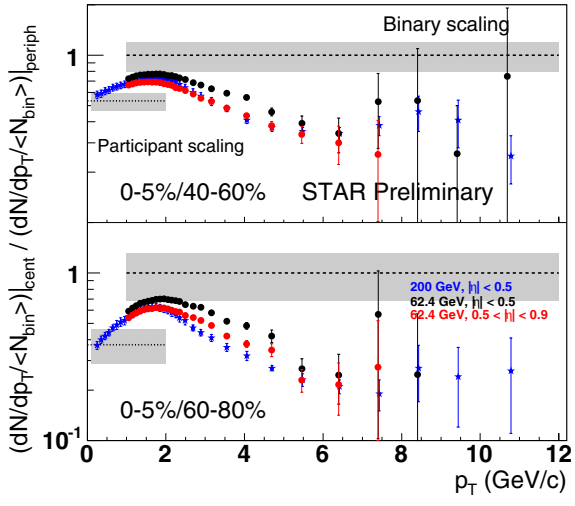

Fig. 3. Preliminary R_{CP} measurements at 62 GeV (circles) for two different pseudorapidity regions are compared to previous results at 200 GeV (stars) [3]

ditional dE/dx particle identification, time-of-flight techniques, and dE/dx measurements in the relativistic rise region provide $\pi^{\pm}$ identification up to $p_{\rm T} \sim 7$ GeV/c [17]. At $p_{\rm T} \sim 3$ GeV/c, R_{CP} for identified $\pi^{\pm}$ is 20% less than that for inclusive charged hadrons from Fig. 3, whereas R_{CP} for identified $\pi^{\pm}$ and inclusive charged hadrons are approximately equal for $p_{\rm T}$ above 5 GeV/c. This implies that the "baryon excesss" that has been seen in 200 GeV Au+Au collisions is also present in 62 GeV collisions [17]. R_{CP} measurements for identified strange particles in 200 GeV d+Au collisions also demonstrate a meson-baryon difference at intermediate $p_{\rm T}$, with relative yields for Λ and Ξ in central d+Au collisions that are similar to each other and larger than the relative yields for

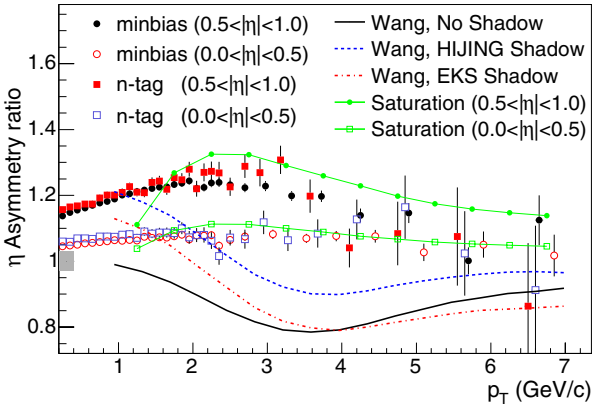

Fig. 4. Ratios of the inclusive charged hadron yield in d+Au collisions measured in the Au beam direction to the yield measured in the deuteron beam direction for minimum-bias collisions and for collisions where the neutron in the deuteron was a spectator [20]

K^0_S and ϕ [18]. STAR has also measured the inclusive π^0 yield in d+Au collisions up to $p_{\rm T} \sim 15$ GeV/c [19].

Recently, STAR has also investigated the pseudorapidity (η) dependence of inclusive charged hadron yields in d+Au collisions. Figure 4 shows the ratios of the yield in the Au beam ($\eta < 0$) direction to that in the deuteron beam ($\eta > 0$) direction [20], together with predictions from pQCD and gluon saturation calculations. At intermediate $p_{\rm T}$, the pQCD calculations [21] predict a pseudorapidity asymmetry with the sign opposite to that observed in the data, even though the same calculations provide a good description of the total charged particle multiplicity as a function of pseudorapidity [20]. In contrast, the gluon saturation calculations [22] are in qualitative agreement with the data.

3 Azimuthal anisotropies

Azimuthal anisotropies at RHIC are believed to have a hydrodynamic origin at low $p_{\rm T}$, to indicate constituent quark coalescence at intermediate $p_{\rm T}$, and to arise from partonic energy loss at high $p_{\rm T}$. Figure 5 shows the azimuthal anisotropy of charged hadrons, characterized by the second Fourier component of the azimuthal distribution v_2, for intermediate impact parameter Au+Au collisions at 200 GeV [23]. Results are shown from three different techniques to calculate v_2: two-particle cumulants, four-particle cumulants, and the difference between the observed two-particle correlations in Au+Au and pp collisions. Each technique has a different sensitivity to systematic effects associated with flow fluctuations and non-flow effects. Results from a modified reaction-plane technique, in which charged particles within $|\Delta\eta| < 0.5$ of the leading charged hadron are excluded from the calculation of the reaction plane, are essentially identical to those found from the difference between Au+Au and pp two-particle correlations [24]. The "true" v_2 is believed to fall between the two- and four-particle cumulant results. The data show

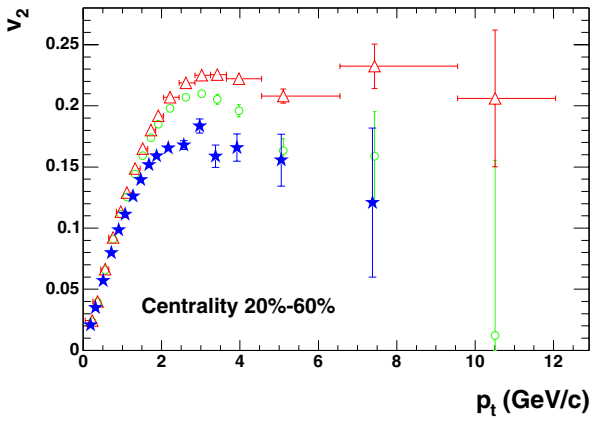

Fig. 5. $v_2(p_T)$ of charged particles in 200 GeV Au+Au collisions obtained using the two-particle cumulant method (triangles), the four-particle cumulant method (stars), and the difference between two-particle correlation measurements in Au+Au and pp collisions (circles) [23]

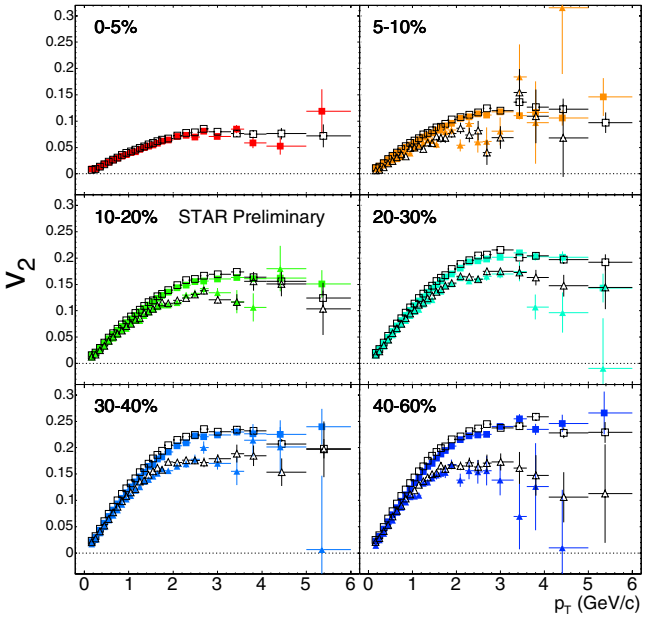

Fig. 6. $v_2(p_T)$ of charged hadrons as a function of centrality for 62 GeV (solid points, preliminary) and 200 GeV (open points, from [24]) Au+Au collisions. Both two-particle cumulant (squares) and four-particle cumulant (triangles) comparisons are shown

that v_2 is non-zero at least up to $p_T \sim 8$ GeV/c, well into the region where parton fragmentation is believed to dominate hadron production.

Figure 6 shows a comparison between the observed $v_2(p_T)$ in 62 and 200 GeV Au+Au collisions. Both two-particle and four-particle cumulant results are shown at each energy. The two-particle and four-particle v_2 values typically differ by $\sim$20%. The 62 and 200 GeV results nonetheless agree to within a few percent for all p_T and centralities, indicating that the physical origins of azimuthal anisotropy are unchanged over this energy span.

4 Di-hadron correlations

Partonic energy loss should induce a characteristic path-length dependence on jet quenching observables [25]. This can be studied by observing high-p_T di-hadron angular correlations with respect to the reaction plane. Previous STAR results [5,6] show that near-side angular distributions between high-p_T trigger particles and intermediate-p_T associated particles contain jet-like correlations in pp, d+Au and Au+Au collisions. Similarly, back-to-back angular distributions in pp, d+Au and peripheral Au+Au collisions show peaks at $\Delta\phi = \pi$ that are characteristic of di-jets, but these are absent in central Au+Au collisions. Figure 7 shows the measured di-hadron azimuthal distributions of associated particles with $2\text{GeV}/c < p_T^{\text{assoc}} < p_T^{\text{trig}}$ when trigger particles with $4 < p_T^{\text{trig}} < 6$ GeV/c are located in or out of the reaction plane [23]. The distributions follow the elliptic flow expectations, with enhancements at $\Delta\phi = 0$ and π. After elliptic flow subtraction, the near-side distributions are consistent with those seen in pp collisions. The back-to-back distributions are suppressed in Au+Au collisions and the out of plane distribution, which involves a longer path length through the dense medium, is suppressed more strongly. Future high statistics measurements like this one will provide a detailed experimental determination of the path-length dependence of jet quenching.

Figure 8 shows a comparison between the observed di-hadron azimuthal distributions in 62 and 200 GeV Au+Au collisions. PYTHIA predicts that the near-side yield should be a factor of $\sim$3 smaller in 62 GeV pp collisions than in

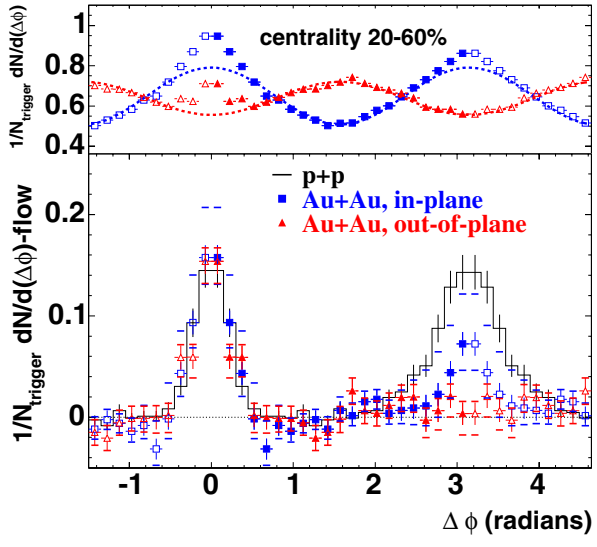

Fig. 7. Azimuthal distribution of associated particles when trigger particles are in plane (squares) and out of plane (triangles) for 200 GeV Au+Au collisions [23]. Open symbols are reflections of the solid symbols about $\Delta\phi = 0$ and π. The upper panel shows the observed distributions, together with the elliptic flow expectations, and the lower panel shows results after subtracting elliptic flow. The histogram shows the azimuthal distribution from pp collisions

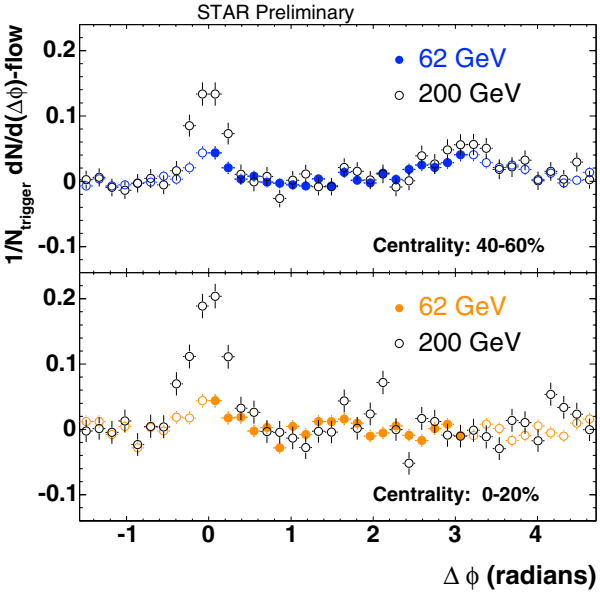

Fig. 8. Preliminary di-hadron azimuthal distributions for $4 < p_{\rm T}^{\rm trig} < 6$ GeV/c, $2{\rm GeV}/c < p_{\rm T}^{\rm assoc} < p_{\rm T}^{\rm trig}$, and $|\eta| < 0.9$, in 62 and 200 GeV Au+Au collisions. Elliptic flow, determined with the modified reaction-plane method, has been subtracted

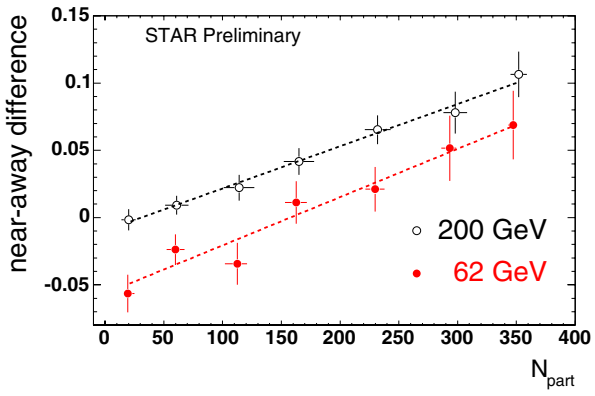

Fig. 9. Preliminary difference in the near-side ($|\Delta\phi| < 0.8$) and back-to-back ($|\Delta\phi - \pi| < 0.8$) di-hadron yields as a function of the number of participants for $4 < p_{\rm T}^{\rm trig} < 6$ GeV/c, $2{\rm GeV}/c < p_{\rm T}^{\rm assoc} < p_{\rm T}^{\rm trig}$, $|\eta| < 0.9$, in 62 and 200 GeV Au+Au collisions. The dashed lines show linear fits to the data

200 GeV collisions [26], primarily due to the softer partonic spectrum at the lower energy. PYTHIA also predicts that the back-to-back yields should be similar at the two energies. The data are consistent with both of these expectations. But it should be noted that, given the strong suppression of the back-to-back yield that is observed in central Au+Au collisions at 200 GeV [5], this indicates that the back-to-back yield is also strongly suppressed at 62 GeV. Figure 9 provides an alternative way to evaluate parton interactions in the dense medium. The difference in yields on the near and away sides cancels any elliptic flow contribution to the background, significantly reducing the systematic uncertainties. At 200 GeV the difference is small for peripheral collisions, indicating that the associated particle yields on the near and away sides are comparable. In contrast, at 62 GeV the significant reduction in the near-side yield leads to a negative difference for peripheral collisions. The changes in the near-away differences as a function of participant number are very similar at the two energies, which indicates that the interactions of the "associated" parton in the dense medium are similar at the two energies.

Very recently, STAR has extended studies of jet- and di-jet-like di-hadron azimuthal distributions to include all associated particles, independently of $p_{\rm T}$ [27]. Figure 10 shows the associated particle distributions, as well as the relative yields of associated particles in Au+Au collisions versus pp collisions. The back-to-back yields at $p_{\rm T}^{\rm assoc} > 2$ GeV/c are suppressed, consistent with the previous measurement [5], but at low $p_{\rm T}^{\rm assoc}$ the associated particle yields are strongly enhanced. This is consistent with partonic energy loss models, which require the soft radiated gluons to contribute to particle production. One is tempted to identify all of the associated particles on the away side with the fragments of the original energetic parton. However, this interpretation should not be taken too literally because (a) the observed distribution of away-side hadrons is very close to that one would obtain simply by conserving transverse momentum in the presence of the trigger hadron [27,28], and (b) the total associated energy on the away side may exceed that on the near side, indicating that a sizable amount may be contributed by the medium [27]. Figure 11 shows the $\langle p_{\rm T} \rangle$ of the associated hadrons on the away side as a function of centrality.

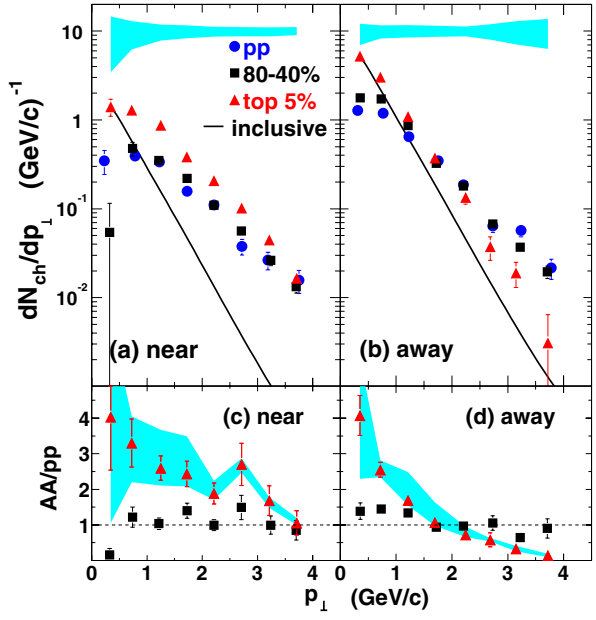

Fig. 10. Associated charged hadron $p_{\rm T}$ distributions and AA/pp ratios on the near ($|\Delta\phi| < 1$) and away ($|\Delta\phi| > 1$) sides for $4 < p_{\rm T}^{\rm trig} < 6$ GeV/c, in 200 GeV pp and Au+Au collisions [27]. The bands show the systematic uncertainties for central Au+Au collisions and the lines show the inclusive spectral shape

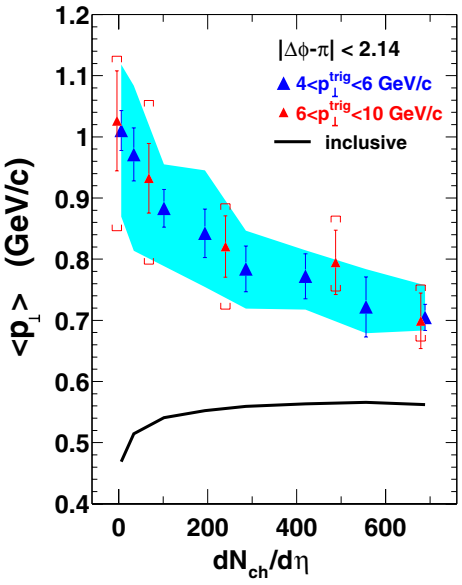

Fig. 11. Away-side associated charged hadron $\langle p_T \rangle$ as a function of centrality for $4 < p_T^{trig} < 6$ GeV/c (band shows systematic errors) and for $6 < p_T^{trig} < 10$ GeV/c (caps show systematic errors) [27]. The left-most points are from pp collisions. The curve shows the $\langle p_T \rangle$ of the inclusive charged hadron distribution

In pp and peripheral Au+Au collisions, the $\langle p_T \rangle$ of the associated hadrons is much larger than that of the inclusive charged hadron distribution. However, the $\langle p_T \rangle$ of the associated hadrons drops as the collisions become more central, whereas that of the inclusive distribution increases, so the difference is much smaller for central Au+Au collisions. A similar behavior is observed for both p_T^{trig} regions. These results may indicate a progressive equilibration of the associated hadrons with the bulk medium from peripheral to central collisions.

Figure 10 indicates that the near-side associated particle yield is much larger in central Au+Au collisions than in pp collisions, even for relatively large p_T^{assoc}. This appears to contradict the observation of similar near-side yields in pp, d+Au, and Au+Au collisions reported in [5,6]. The difference arises primarily from different treatments of the η acceptance of the STAR detector. The analyses in [5,6] adopted a limited η region. In contrast, the analysis in Fig. 10 attempts to integrate all associated hadrons on the near side, even those that are widely separated from the trigger hadron in pseudorapidity. We now recognize that there are two separate contributions to the near-side associated hadrons — a short-range, jet-like peak which is Gaussian in $|\Delta\eta|$ and a long-range component that extends at least to $|\Delta\eta| > 1.5$.

5 Forward physics in d+Au

The BRAHMS Collaboration has reported that negative hadron production in the forward direction is strongly suppressed in d+Au collisions relative to pp collisions [11].

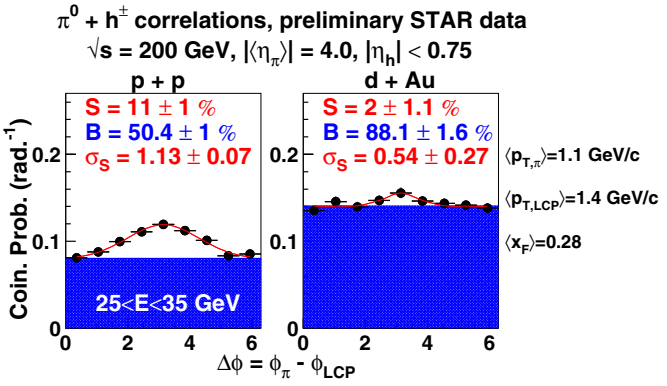

Fig. 12. Preliminary azimuthal distributions of leading charged hadrons in 200 GeV pp and d+Au collisions at midrapidity ($|\eta| < 0.75$, $p_T > 0.5$ GeV/c) in coincidence with identified π^0 at $\langle \eta \rangle = 4.0$ [31]

This result may provide evidence at RHIC for the onset of gluon saturation at small-x in the Au nucleus. In a pQCD calculation, the x values sampled by the BRAHMS measurement are not particularly small, which casts doubt on the saturation explanation, but traditional shadowing appears insufficient to explain the data [29]. Thus, it's important to explore the particle production mechanisms in the forward direction to see if other effects might lead to the observed suppression.

STAR measurements [30,31] have shown that the inclusive π^0 production cross sections in 200 GeV pp collisions at $\langle \eta \rangle = 3.8$ and 3.3 are well described by pQCD calculations, in constrast to forward particle yields at comparable p_T in lower energy collisions [32]. To provide better understanding of forward particle production, STAR has measured charged hadrons at midrapidity that are associated with an energetic π^0 in the forward direction. Figure 12 shows the back-to-back angular correlations observed in pp and d+Au collisions [31]. The pp data show an enhancement in the back-to-back yield, consistent with PYTHIA predictions for di-jet production. HIJING predicts that a similar enhancement should be present in d+Au collisions, but Fig. 12 shows that very little correlated back-to-back yield is visible for π^0 energies in the range $25 < E_\pi < 35$ GeV. In contrast, back-to-back peaks of similar strength are observed in pp and d+Au collisions for $35 < E_\pi < 45$ GeV. The changing behavior of the d+Au correlation strength with E_π is consistent with the general expectations of saturation, but the current statistics are quite limited and more data are called for. For a detailed discussion of forward particle production measurements with STAR, see [33].

6 Conclusion

In conclusion, recent high-p_T results from STAR show that jet quenching, elliptic flow and di-hadron correlation measurements in Au+Au collisions at $\sqrt{s_{NN}} = 62$ GeV are very similar to previous results from 200 GeV Au+Au collisions. The meson-baryon differences that have been

seen at intermediate p_T in 200 GeV Au+Au collisions are also present in 62 GeV Au+Au collisions and in 200 GeV d+Au collisions. Measurements in 200 GeV d+Au collisions of the backward-forward inclusive hadron yield asymmetries and of forward-midrapidity di-hadron correlations are qualitatively consistent with the gluon saturation model.

A host of new high-p_T results from STAR are expected shortly, based on the analysis of the high-statistics 200 GeV Au+Au data that were taken during Run 4 and of the Cu+Cu data that have been taken in Run 5.

References

1. M. Gyulassy, M. Plumer, Phys. Lett. B **243**, 432 (1990); X.N. Wang, M. Gyulassy, Phys. Rev. Lett. **68**, 1480 (1992)
2. C. Adler et al. (STAR Collaboration), Phys. Rev. Lett. **89**, 202301 (2002)
3. J. Adams et al. (STAR Collaboration), Phys. Rev. Lett. **91**, 172302 (2003)
4. K. Adcox et al. (PHENIX Collaboration), Phys. Rev. Lett. **88**, 022301 (2002); S.S. Adler et al. (PHENIX Collaboration), Phys. Rev. Lett. **91**, 072301 (2003)
5. C. Adler et al. (STAR Collaboration), Phys. Rev. Lett. **90**, 082302 (2003)
6. J. Adams et al. (STAR Collaboration), Phys. Rev. Lett. **91**, 072304 (2003)
7. J. Adams et al. (STAR Collaboration), Rev. Lett. **92**, 052302 (2004)
8. S.S. Adler et al. (PHENIX Collaboration), Phys. Rev. Lett. **91**, 172301 (2003)
9. M.A.C. Lamont et al. (STAR Collaboration), J. Phys. G **30**, S963 (2004); J. Castillo et al. (STAR Collaboration), J. Phys. G **30**, S1207 (2004)
10. V. Greco et al., Phys. Rev. Lett. **90**, 202302 (2003); R.J. Fries et al., Phys. Rev. Lett. **90**, 202303 (2003); R.C. Hwa, C.B. Yang, Phys. Rev. C **67**, 064902 (2003); D. Molnar, S.A. Voloshin, Phys. Rev. Lett. **91**, 092301 (2003)
11. I. Arsene et al. (BRAHMS Collaboration), Phys. Rev. Lett. **93**, 242303 (2004)
12. J. Adams et al. (STAR Collaboration), nucl-ex/0501009
13. K.H. Ackermann et al. (STAR Collaboration), Nucl. Instrum. Meth. **A499**, 624 (2003)
14. M.M. Aggarwal et al. (WA98 Collaboration), Phys. Rev. Lett. **81**, 4087 (1998); **84**, 578(E) (2000)
15. D. d'Enterria, Eur. J. Phys. C **43** (2005)
16. X.N. Wang, Phys. Lett. B **579**, 299 (2004)
17. Z. Xu et al. (STAR Collaboration), nucl-ex/0411001
18. P.G. Jones et al. (STAR Collaboration), J. Phys. G **31**, S399 (2005)
19. A. Mischke et al. (STAR Collaboration), Eur. J. Phys. C **43** (2005)
20. J. Adams et al. (STAR Collaboration), Phys. Rev. C **70**, 064907 (2004)
21. X.N. Wang, Phys. Lett. B **565**, 116 (2003)
22. D. Kharzeev, Y.V. Kovchegov, K. Tuchin, Phys. Lett. B **599**, 23 (2004); D. Kharzeev, K. Tuchin private communication
23. J. Adams et al. (STAR Collaboration), Phys. Rev. Lett. **93**, 252301 (2004)
24. J. Adams et al. (STAR Collaboration), nucl-ex/0409033
25. R. Baier, D. Schiff, B.G. Zakharov, Annu. Rev. Nucl. Part. Sci. **50**, 37 (2000)
26. K. Filimonov, J. Phys. G **31**, S513 (2005)
27. J. Adams et al. (STAR Collaboration, nucl-ex/0501016
28. N. Borghini, P.M. Dinh, J.-Y. Ollitrault, Phys. Rev. C **62**, 034902 (2000)
29. V. Guzey, M. Strikman, W. Vogelsang, Phys. Lett. B **603**, 173 (2004)
30. J. Adams et al. (STAR Collaboration), Phys. Rev. Lett. **92**, 171801 (2004)
31. A. Ogawa et al. (STAR Collaboration), nucl-ex/0408004
32. C. Bourrely, J. Soffer, Eur. Phys. J. C **36**, 371 (2004)
33. L.C. Bland et al., Eur. Phys. J. C **43** (2005)